

Molecular reorientation of a nematic glass by laser-induced heat flow

R. Elschner, R. Macdonald, and H. J. Eichler

Optisches Institut, Technische Universität Berlin, Hardenbergstraße 36, D-10623 Berlin, Germany

S. Hess

Institut für Theoretische Physik, Technische Universität Berlin, Hardenbergstraße 36, D-10623 Berlin, Germany

A. M. Sonnet

Dipartimento di Ingegneria Chimica, Università di Napoli Federico II, Piazzale Tecchio 80, I-80125 Naples, Italy

(Received 25 November 1998)

Laser-induced birefringence patterns which break the symmetry of the experimental setup have been observed in a low molar mass anisotropic glass with nematic orientational order under a polarizing microscope. It is shown that the observed spatial modulations in birefringence can be explained by laser-induced heat flow and stress, leading to molecular reorientation which is then frozen and stored in the glassy state if the optical excitation is switched off. The experimental findings can be regarded as a manifestation of heat-flow alignment caused by a spatially inhomogeneous temperature field. [S1063-651X(99)16805-3]

PACS number(s): 42.70.Df, 61.30.Cz, 61.30.Gd

I. INTRODUCTION

Since the mid-1980s it has been recognized that besides liquid crystalline polymers some low molar mass liquid crystals may also form a glassy state at room temperature even by cooling at usually slow rates of some few Kelvins per minute [1]. In particular, a binary mixture of two β -naphthylesters was shown to exhibit an anisotropic glassy state at temperatures below $T_g = 310$ K which results from freezing of nematic orientational order. Generally, liquid crystalline glasses offer a promising combination of unique optical and other physical properties of ordered mesophases together with excellent mechanical and fabrication properties of noncrystalline organic materials. As an example, it was demonstrated [2,3] that photothermal excitation can be successfully applied for reversible holographical storages. Lifetimes for stored holographic gratings of several years have been obtained and more than 1000 writing, reading, and erasure cycles have been realized without any dramatic decrease in diffraction efficiency on the same spot of the sample [4]. These optical storage effects have been attributed mainly to structural relaxation processes affecting the local birefringence and refractive indices via the mass density ρ and the scalar order parameter S following photothermal excitation [5].

It is the main purpose of the present paper to discuss how light absorption and laser-induced local heating in these new nematic low molar glasses may cause also molecular reorientations and rotations of the optical axis, which has been experimentally verified with the help of polarization microscopy. The observed birefringence patterns are intriguing because they break the symmetry of the experimental arrangement. It will be shown that the reorientation phenomena can be explained by stress-optical coupling similar to stress-induced birefringence [6], where the stress is caused by a locally inhomogeneous temperature field. There are close analogies to well known flow alignment [7–9] or birefringence but without the need of any material flow. From a

more phenomenological point of view, the experimental findings can be regarded as a manifestation of a heat-flow birefringence [10–13] caused by a spatial dependence of the temperature field. The microscopic mechanisms responsible for similar effects in gases [10–12] and ordinary liquids [13], however, differ from those which are relevant in the glasses considered here. In particular, the dynamics even of isotropic glasses are rather complex [14–16], and can be expected to be more complicated in liquid crystalline glasses. Consequently, the present work discusses the effect under quasi-stationary conditions.

This paper proceeds as follows: In Sec. II, the experimental setup and observations are presented and discussed in more detail. In Sec. III, a theoretical model based on an equation valid for both the liquid crystalline nematic and isotropic phases is developed for the second rank alignment tensor which is associated with the optical birefringence. A coupling of the alignment tensor with the symmetric traceless part of the pressure tensor (stress tensor) is considered by introducing a stress-optical coefficient. This equation is then specialized for a uniaxial alignment with a constant scalar order parameter. In Sec. IV, this equation is applied to the experimental situation. First, the pressure tensor is calculated starting from a local stability criterion and an appropriate ansatz for the temperature field. The reorientation of the nematic director field is then calculated analytically for small reorientation angles and numerically for the general case. In Sec. V, the experimental observations are compared to the theoretical predictions, and some concluding remarks are given.

II. EXPERIMENT

The investigations were performed with a 10- μ m-thick nematic film of an eutectic mixture of two β -naphthylesters [1], which has been described in more detail in Refs. [2,3]. The phase sequences of the mixture are crystalline \rightarrow (409 K) \rightarrow nematic \rightarrow (413 K) \rightarrow isotropic. At usual

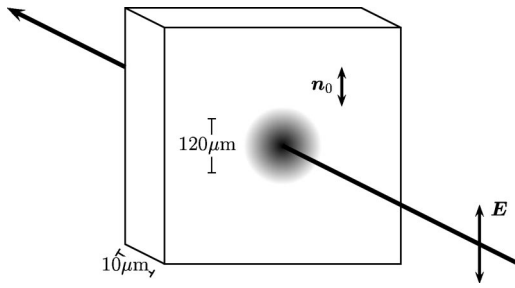


FIG. 1. Experimental setup. The sample is illuminated by a laser with the polarization parallel to the initial director orientation n_0 .

cooling rates of a few K/min, however, crystallization is avoided and the material undergoes a glass transition at 310 K. Consequently, the orientational order of the nematic phase is frozen and the glassy state is anisotropic. The material was doped with a small amount (0.1%) of a dichroic anthraquinone dye (D37, BDH) to enhance the absorption and to achieve laser heating. It should be noted, however, that similar effects to those described below have also been observed in samples where optical heating was achieved by an additional metallic layer on one of the inner container surfaces [17].

The sample was sandwiched between two 1-mm-thick glass plates, which were separated by Mylar spacers. The inner surfaces of the plates were coated with a rubbed polymer to accomplish the desired homogeneous planar alignment. The cells were filled with the material in the isotropic phase, i.e., above the clearing point $T_{NI}=413$ K. A nematic orientation of the glassy material along the rubbing direction was then achieved by slow (2 K/min) cooling down to a temperature where the high viscosity of the glass appears (≈ 360 K). After that, the nematic alignment was frozen by faster (100 K/min) cooling into the glassy state.

A focused argon-ion laser beam ($\lambda=514$ nm), which was modulated with a pockels cell, was used for the thermo-optical excitation. The $1/e$ radius r_0 of the intensity profile of the beam was measured to $r_0=60$ μm . The sample was illuminated with a single pulse of 20-ms duration on each spot at a temperature of 293 K. The incident polarization of the laser beam was parallel to the initial director field; see Fig. 1. The absorbed intensity leads to rapid laser heating due to radiationless recombination processes in the dye molecules. It was shown that after thermal excitation, a modulation in properties such as density or order parameter is frozen and remains in the optically heated region, because the structural relaxation back in a lower temperature state is incomplete [5]. As a result, the optical properties connected with density and orientational order, mainly the birefringence, are modulated and frozen as well, which has been successfully applied for holographic grating recording. In a single beam experiment as discussed above, a laser-induced lens [18] with perfect radial symmetry has been obtained at moderate light intensities (<150 W/cm^2), which was proved under a polarizing microscope as well as by diffraction of the laser beam.

However, for higher excitation intensities (>150 W/cm^2), diffraction at the induced lens was more complex, and spatial patterns inside the stored lenses were observed with the help of the polarization microscope; see Fig. 2. The patterns ap-

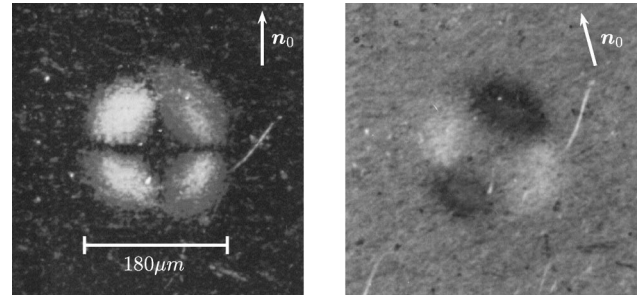


FIG. 2. Polarization patterns of the frozen-in reorientation. In the left picture the crossed nichols are parallel to the initial director orientation, while for the right image the sample has been rotated by 15° .

pear different by rotating the sample between crossed polarizers: If the angle ψ between the optical axis of the sample and the analyzer is zero, the spot is divided into four parts of equal brightness and color, with a Maltesian-like cross along the polarizer and analyzer axes. For all $\psi \neq 0, \pi/2, \dots$, quarters of two different colors have been observed which are in contrast to the surrounding area. The pattern is then centrosymmetric, where the opposite quarters behave equal. Especially for a rotation $\psi \rightarrow -\psi$, the quarters exchange their colors.

These observations can be explained if we assume that the optical axis within the quarters is rotated around the sample normal, as will be discussed in Sec. III. They are therefore manifestations of molecular reorientation effects caused by the above mentioned laser heating which occur in addition to the modulation in density and order parameter under certain circumstances.

III. THEORETICAL MODEL FOR THE HEAT FLOW ALIGNMENT

A. Equation for the alignment tensor

The molecular orientation is described by the second rank alignment tensor

$$\mathbf{a} := \sqrt{15/2} \langle \hat{\mathbf{u}}\hat{\mathbf{u}} \rangle, \quad (1)$$

where \mathbf{u} is a unit vector parallel to the figure axis of an effectively uniaxial molecule. The symbol $\langle \cdot \rangle$ indicates the symmetric-traceless part of a tensor, e.g., $\hat{\mathbf{u}}\hat{\mathbf{u}} = \mathbf{u}\mathbf{u} - \frac{1}{3}\delta$, where δ is the unit tensor. The bracket $\langle \cdot \cdot \cdot \rangle$ stands for an average over the molecular orientations. Phenomenologically, the alignment tensor can be introduced by

$$\vec{\epsilon} = \epsilon_a \mathbf{a}, \quad (2)$$

where $\vec{\epsilon}$ is the symmetric traceless part of the dielectric tensor which gives rise to birefringence. The coefficient ϵ_a characterizes the magnitude of the optical anisotropy.

In particular, in the uniaxial nematic phase in equilibrium, one has

$$\mathbf{a} = \sqrt{\frac{3}{2}} a_{\text{eq}} \hat{\mathbf{n}}\hat{\mathbf{n}}, \quad (3)$$

with the director \mathbf{n} ($\mathbf{n} \cdot \mathbf{n} = 1$) and the magnitude $\text{tr}(\mathbf{a}^2) = a_{\text{eq}}^2$ of the alignment tensor, where $a_{\text{eq}} = \sqrt{5}S$ with the Maier-Saupe order parameter $S = \langle P_2(\mathbf{u} \cdot \mathbf{n}) \rangle$.

The point of departure for the present considerations is the equation of change for \mathbf{a} :

$$\frac{\partial}{\partial t} \mathbf{a} + \tau_a^{-1} (\mathbf{\Phi} - \xi_0^2 \Delta \mathbf{a} - \tilde{\mathbf{C}} \tilde{\mathbf{P}}) = \mathbf{0}, \quad (4)$$

where $\mathbf{\Phi} = A(T) \mathbf{a} \cdot \dots \cdot \vec{\mathbf{a}} \cdot \vec{\mathbf{a}} + \dots \cdot \text{tr}(\mathbf{a}^2) \mathbf{a}$ is the derivative of a Landau-de Gennes potential with respect to the alignment tensor. Here $A(T) = 1 - T^*/T$, and the ellipses stand for characteristic coefficients approximately independent of the temperature; T^* is somewhat below the isotropic-nematic transition temperature.

In Eq. (4), $\tilde{\mathbf{P}}$ is the symmetric traceless part of the pressure tensor \mathbf{P} . It is linked with the stress tensor $\boldsymbol{\sigma}$ by $\mathbf{P} = -\boldsymbol{\sigma}$. An explicit expression for $\tilde{\mathbf{P}}$ as a function of the temperature field will be given in Sec. III. The relaxation time τ_a and the length ξ_0 are considered as phenomenological coefficients.

In a stationary state and when the spatial variation of \mathbf{a} can be disregarded, one has $\mathbf{\Phi} = \tilde{\mathbf{C}} \tilde{\mathbf{P}}$. Then, in the isotropic phase where the terms nonlinear in the alignment tensor are negligible, one has, for $T > T^*$,

$$\mathbf{a} = A(T)^{-1} \tilde{\mathbf{C}} \tilde{\mathbf{P}}, \quad (5)$$

with a typical pretransitional increase of the coupling proportional to $(T - T^*)^{-1}$ [19]. For $T \gg T^*$, this implies

$$\tilde{\boldsymbol{\epsilon}} = \epsilon_a \mathbf{a} = \epsilon_a \tilde{\mathbf{C}} \tilde{\mathbf{P}} = -2\nu C \tilde{\mathbf{P}}, \quad (6)$$

where $\nu = \frac{1}{2}(\nu_{\parallel} + \nu_{\perp})$ is an average index of refraction, and C is the standard stress optical coefficient, e.g., used for polymeric materials. There, a typical value is $2C \approx -10^{-8} \text{ Pa}^{-1}$ [6]. With $\nu \approx 1$ and $\epsilon_a \approx 0.1$, this yields the estimate $\tilde{\mathbf{C}} \approx -10^{-7} \text{ Pa}^{-1}$.

In an isotropic liquid one has $\tilde{\mathbf{P}} = -2\eta \vec{\nabla} \mathbf{v}$, where \mathbf{v} is the flow velocity and η is the (shear) viscosity. Then Eq. (4) becomes equivalent to an equation of change for the alignment tensor derived previously within the framework of irreversible thermodynamics [20,21] and from a Fokker-Planck equation [22] when the coefficient $\tilde{\mathbf{C}}$ is linked with a coupling relaxation time coefficient τ_{ap} by

$$2\tilde{\mathbf{C}} \eta = \sqrt{2} \tau_{ap}. \quad (7)$$

The theory presented in Ref. [20–22] applies to both the isotropic and nematic phases, and allows one to relate the relaxation time coefficients τ_a and τ_{ap} to the Leslie coefficients γ_1 and γ_2 , viz.

$$\gamma_1 = 3a_{\text{eq}}^2 \tau_a \frac{\rho}{m} k_B T, \quad \gamma_2 = 2\sqrt{3} a_{\text{eq}} \tau_{ap} \frac{\rho}{m} k_B T, \quad (8)$$

where ρ is the mass density and m is the mass of a molecule. As a consequence, Eqs. (7) and (8) lead to

$$\tilde{\mathbf{C}} = \left(4 \sqrt{\frac{3}{2}} a_{\text{eq}} \frac{\rho}{m} k_B T \right)^{-1} \frac{\gamma_2}{\eta}, \quad (9)$$

where η , in the case of a nematic liquid crystal, should be identified with the average $\frac{1}{3}(\eta_1 + \eta_2 + \eta_3)$ of the three Miesowicz viscosity coefficients η_1 , η_2 , and η_3 . For a typical nematic liquid crystal one has $\gamma_2/\eta \approx -\frac{3}{2}$, and $a_{\text{eq}} = \sqrt{5}S \approx 1$. With $(\rho/m)k_B T \approx 10^{-6} - 10^{-7} \text{ Pa}$ corresponding to a molecular mass of 2000 or 200, the coefficient $\tilde{\mathbf{C}}$ as given by Eq. (9) has the same sign and a similar order of magnitude as the value stated above for polymeric materials.

Here, we shall apply Eq. (4) to a glassy state where the viscosity η is very large such that a viscous flow is suppressed. The coefficient γ_2 being equal to the difference between two Miesowicz coefficients, it is likely that the ratio γ_2/η is approximately constant across the glass transition. Thus we assume that $\tilde{\mathbf{C}}$ is of comparable size in the fluid and the glassy state.

B. Change of the director in the glassy nematic

Under equilibrium conditions, the alignment tensor in the nematic phase is determined by $\mathbf{\Phi} = \mathbf{\Phi}(\mathbf{a}) = \mathbf{0}$. This yields a uniaxial equilibrium alignment tensor of the form of Eq. (3), with a temperature dependent order parameter $a_{\text{eq}} \sim S$. Typical values for S are in the range of 0.4–0.7. When the temperature is not too close to the nematic-isotropic transition temperature, one may assume that the uniaxiality and the magnitude of the alignment are not affected by spatial variations and orienting torques. Then Eq. (4) reduces to

$$\sqrt{\frac{3}{2}} a_{\text{eq}} \left(\tau_a \frac{\partial}{\partial t} - \xi_0^2 \Delta \right) (\mathbf{nn}) - \tilde{\mathbf{C}} \tilde{\mathbf{P}} = \mathbf{0}, \quad (10)$$

where it is understood that this equation has to be solved under the constraint $\mathbf{n} \cdot \mathbf{n} = 1$.

Scalar multiplication of Eq. (10) by \mathbf{n} leads to

$$\gamma_1 \frac{\partial}{\partial t} \mathbf{n} - K \Delta \mathbf{n} - C_{np} \tilde{\mathbf{P}} \cdot \mathbf{n} = \mathbf{0} \quad (11)$$

where, by use of Eq. (8),

$$C_{np} = 2 \sqrt{\frac{3}{2}} a_{\text{eq}} \frac{\rho}{m} k_B T \tilde{\mathbf{C}} \quad (12)$$

was defined, and the characteristic length ξ_0 is seen to be related to an average Frank elasticity coefficient K of a nematic liquid crystal by

$$K = 3a_{\text{eq}}^2 \xi_0^2 \frac{\rho}{m} k_B T. \quad (13)$$

This implies that, in the nematic and liquid phases, ξ_0 is of the order of a molecular length, i.e., $\xi_0 \approx 1 \text{ nm}$. Again, the constraint $\mathbf{n} \cdot \mathbf{n} = 1$ has to be obeyed. Equation (11) for the vector \mathbf{n} is preferred for analytic calculations. For numerical computations, however, Eq. (10) containing the dyadic \mathbf{nn} should be used. It allows the occurrence of typical nematic defects [23–25].

IV. APPLICATION TO THE OPTICAL STORAGE EXPERIMENT

A. Thermal stress

In the glassy state where a flow is suppressed, the local conservation of linear momentum (mechanical stability) requires

$$\nabla \cdot \vec{\mathbf{P}} + \nabla p = \mathbf{0}. \quad (14)$$

Here $p = p(T)$ is the hydrostatic pressure. Due to the local absorption of the laser light shining on the material, there is a local heating which implies a spatial variation of the temperature. Thus one has

$$\nabla p = \left(\frac{\partial p}{\partial T} \right)_V \nabla T \quad (15)$$

where the quantity $(\partial p / \partial T)_V$ can be related to the (cubic) thermal expansion coefficient α , and the isothermal compressibility χ_T by $(\partial p / \partial T)_V = \alpha / \chi_T$. A typical order of magnitude is $(\partial p / \partial T)_V \approx 10^6$ Pa/K.

Next we consider a cylindrical geometry with the axis parallel to the laser beam. For a thin sample (10 μm in the experiment) a spatial variation in the direction of the laser beam can be disregarded. Then all spatial variation is within a plane normal to the beam. By \mathbf{r} we denote a position vector within this plane.

From symmetry arguments one expects that $\vec{\mathbf{P}}$ is of the form

$$\vec{\mathbf{P}} = P(r) \hat{\mathbf{r}} \hat{\mathbf{r}}, \quad (16)$$

with $r = |\mathbf{r}|$ and $\hat{\mathbf{r}} = \mathbf{r}/r$. Insertion of the ansatz (16) into Eq. (14) with $\nabla p = \hat{\mathbf{r}} p'$ yields the ordinary differential equation

$$\frac{2}{3} r^{-3/2} (r^{3/2} P)' = -p' = - \left(\frac{\partial p}{\partial T} \right)_V T' \quad (17)$$

for the function P . The primes denote the differentiation with respect to r . The general solution of Eq. (17) is

$$P(r) = r^{-3/2} \left(c_1 + \frac{9}{4} \int_0^r p(s) \sqrt{s} ds \right) - \frac{3}{2} p(r), \quad (18)$$

and requiring $P(r)$ to stay finite as $r \rightarrow 0$ gives $c_1 = 0$.

We consider stationary temperature profiles of the form $T = T_0 + \delta T f(r)$, where T_0 is the constant temperature of the environment, and δT is the temperature rise in the center of the beam. Such a temperature profile can be assumed since the sample thickness is much smaller than the lateral dimensions of the laser spot. Consequently, the main heat flow which determines the radial stationary profile is across the film via the semi-infinite glass plates, and lateral diffusion can be neglected [26]. Using Eq. (15), this leads to a scalar pressure of the form $p(r) = p_0 + (\partial p / \partial T)_V \delta T f(r)$.

Two special cases for a temperature profile are used explicitly. First, $T = T_0 + \delta T e^{-(r/r_0)^2}$, where the characteristic length r_0 is of the order of the width of the laser beam. The solution of Eq. (17) is

$$P(r) = \frac{3}{2} \left(\frac{\partial p}{\partial T} \right)_V \delta T \left[\frac{3}{4} \left(\frac{r}{r_0} \right)^{-3/2} \gamma \left(\frac{3}{4}, \left(\frac{r}{r_0} \right)^2 \right) - e^{-(r/r_0)^2} \right], \quad (19)$$

with the incomplete γ function

$$\gamma(\alpha, x) = \int_0^x e^{-s} s^{\alpha-1} ds. \quad (20)$$

This will be used in the numerical treatment presented in Sec. IV C.

Second, the temperature profile

$$T = \begin{cases} T_0 + \delta T \left(1 + 2 \frac{r}{r_c} \right) \left(1 - \frac{r}{r_c} \right)^2, & r \leq r_c \\ T_0, & r \geq r_c, \end{cases} \quad (21)$$

with the finite range r_c is used for the analytic calculation in Sec. IV B. For small r , Eq. (21) is equivalent to a Gaussian profile with $1/e$ radius $r_0 = r_c / \sqrt{3}$.

Solution of Eq. (17), with Eq. (21), leads to

$$P(r) = 18 \left(\frac{\partial p}{\partial T} \right)_V \delta T \left[\frac{1}{7} \left(\frac{r}{r_c} \right)^2 - \frac{1}{9} \left(\frac{r}{r_c} \right)^3 \right] \quad (22)$$

for $r \leq r_c$, and we take $P(r) = 0$ for $r > r_c$. This is motivated by the observation that the unheated glass in the region outside the critical radius remains solidlike. While the function $P(r)$ is allowed to be discontinuous at $r = r_c$, the physically relevant condition $\lim_{r \nearrow r_c} [r^{3/2} P(r)]' = \lim_{r \searrow r_c} [r^{3/2} P(r)]' = 0$ is obeyed at r_c .

B. Analytic calculation of the director field

The essential features of the symmetry breaking molecular reorientation are revealed by an analytic solution for the director field which, however, is only valid for small distortions. In particular, we consider the case $\mathbf{n} = \mathbf{n}_0 + \delta \mathbf{n}$ where \mathbf{n}_0 is constant and $\delta \mathbf{n}$ with $\mathbf{n} \cdot \delta \mathbf{n} = 0$ is a small deviation induced by the thermal pressure $\vec{\mathbf{P}}$, cf. Eq. (22) with Eq. (16). In a stationary situation, Eq. (11) reduces to

$$K \Delta \delta \mathbf{n} + C_{np} \vec{\mathbf{P}} \cdot \mathbf{n}_0 = \mathbf{0}. \quad (23)$$

The ansatz

$$\delta \mathbf{n} = \alpha(r) [(\hat{\mathbf{r}} \cdot \mathbf{n}_0) \hat{\mathbf{r}} - (\hat{\mathbf{r}} \cdot \mathbf{n}_0)^2 \mathbf{n}_0], \quad (24)$$

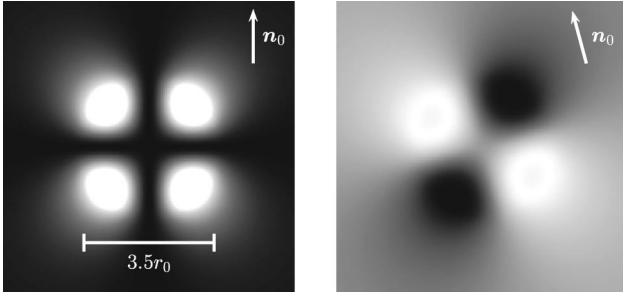


FIG. 3. Density plots of the light intensity generated by the analytical solution for small director reorientations.

and use of Eq. (16) lead to the ordinary differential equation

$$r^{-1}(r\alpha')' - 4r^{-2}\alpha = -\frac{C_{np}}{K}P(r). \quad (25)$$

The solution is

$$\alpha(r) = \frac{1}{42}\alpha_0 g\left(\frac{r}{r_c}\right), \quad (26)$$

with

$$\alpha_0 = r_c^2 \frac{C_{np}}{K} \left(\frac{\partial p}{\partial T}\right)_V \delta T = \left(\sqrt{\frac{3}{2}a_{\text{eq}}}\right)^{-1} \left(\frac{r_c}{\xi_0}\right)^2 \tilde{C} \left(\frac{\partial p}{\partial T}\right)_V \delta T. \quad (27)$$

The function $g(x)$ is given by

$$g(x) = \begin{cases} 4x^5 - 9x^4 + \frac{13}{2}x^2, & x \leq 1 \\ \frac{3}{2}x^{-2}, & x > 1. \end{cases} \quad (28)$$

The homogeneous solutions proportional to r^2 for $r > r_c$ and to r^{-2} for $r < r_c$ have been chosen such that α and its first derivative are continuous at $r = r_c$. The maximum of the function g , occurring at $x \approx 0.810$ is $g_{\text{max}} \approx 1.785$. Thus with the estimate for the order of magnitude of \tilde{C} and $(\partial p/\partial T)_V$ given above, with $\sqrt{3/2}a_{\text{eq}} \approx 1$ and $\delta T \approx 1$ K, one has, for the maximum value α_{max} of $|\alpha(r)|$,

$$\alpha_{\text{max}} \approx 10^{-3} \left(\frac{r_c}{\xi_0}\right)^2. \quad (29)$$

A typical value for r_c is $\approx 100 \mu\text{m}$. The Frank elasticity coefficient $K \sim \xi_0^2$ in the glassy state is expected to be considerably larger than in the fluid nematic phase, where $\xi_0 \approx 1$ nm. The estimates $\xi_0 \approx 1$ or $10 \mu\text{m}$ lead to $\alpha_{\text{max}} \approx 10$ and 10^{-1} , respectively. In the first case, the assumption that the distortion of the director field is small is no longer true; then the solution to Eq. (10) can be found numerically, cf. Sec. IV C.

The intensity transmitted through a sample between crossed polarizer and analyzer, oriented parallel to the unit vectors e^p and e^q , is proportional to

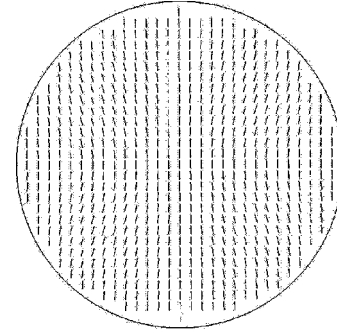


FIG. 4. Director field of the numerical solution. At the circular boundary the alignment is fixed to the initial orientation \mathbf{n}_0 .

$$I = \sin^2(\delta\phi), \quad \delta\phi = \frac{2\pi L}{\lambda} \delta\epsilon, \quad (30)$$

$$\delta\epsilon = e^p \cdot \tilde{\epsilon} \cdot e^q = \epsilon_a \sqrt{\frac{3}{2}} a_{\text{eq}} (e^p \cdot \mathbf{n})(e^q \cdot \mathbf{n}). \quad (31)$$

Here $\delta\phi$ denotes the optical phase shift, L is the thickness of the sample, and λ is the wavelength of the light. With $\phi_0 = (2L/\lambda)\epsilon_a\sqrt{3/2}a_{\text{eq}}$, a quantity which is of the order of 1 in the experiments, the phase shift becomes

$$\delta\phi = \phi_0 \pi (e^p \cdot \mathbf{n})(e^q \cdot \mathbf{n}). \quad (32)$$

For the case of a small distortion of the director field, where $\mathbf{n} = \mathbf{n}_0 + \delta\mathbf{n}$ with $\delta\mathbf{n}$ given by Eq. (24), one obtains

$$\begin{aligned} \delta\phi &= \phi_0 \pi [(e^p \cdot \mathbf{n}_0)(e^q \cdot \mathbf{n}_0) + (e^p \cdot \mathbf{n}_0)(e^q \cdot \delta\mathbf{n}) \\ &\quad + (e^q \cdot \mathbf{n}_0)(e^p \cdot \delta\mathbf{n})] \\ &= \phi_0 \pi \left(\frac{1}{2} \sin 2\psi + \alpha \hat{x} \hat{y} \cos 2\psi \right), \end{aligned} \quad (33)$$

where $-\psi$ is the angle between the direction of the polarizer and \mathbf{n}_0 (i.e. $\mathbf{n}_0 \cdot e^p = \cos \psi$ and $\mathbf{n}_0 \cdot e^q = \sin \psi$), and \hat{x} and \hat{y} are the components of $\hat{\mathbf{r}}$ parallel and perpendicular to \mathbf{n}_0 . Density plots of the resulting intensity with α according to Eq. (26) are given in Fig. 3.

C. Numerical solution

In order also to calculate the equilibrium solutions of Eq. (10) in the general case of large distortions, a numerical algorithm based on a finite difference scheme was used. It is described in detail in Ref. [23,24]. Its main advantage is that it conforms to the nematic symmetry $\hat{\mathbf{n}} \hat{=} -\mathbf{n}$.

A Gaussian temperature profile was assumed, and accordingly $P(r)$ as given by Eq. (19) was used. In order to model the kind of threshold behavior observed in the experiment, where the effect takes place in a region of diameter $\approx 3r_0$, fixed boundary conditions were used. Thus, while in the analytical calculations presented in Sec. IV B the pressure was frozen in, here the alignment is assumed to be fixed outside the heated region.

As can be seen from Eq. (11), the type of equilibrium solution depends on how the ratio $\kappa := K/C_{np}$ compares to the magnitude of the pressure tensor multiplied by the area

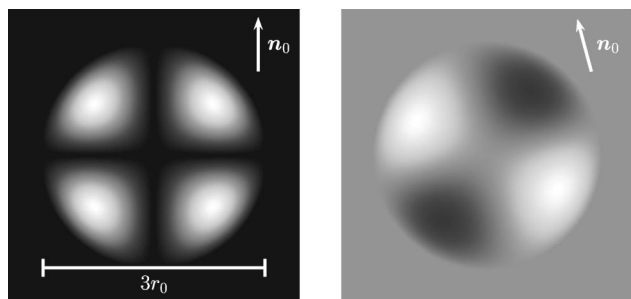


FIG. 5. Simulated polarization patterns for the numerically calculated director field.

of the illuminated spot. For the given experimental setup and with $(\partial p/\partial T)_V \approx 10^6$ Pa/K, this latter product is roughly 0.25 N. On the one hand, the elastic term stabilizes a uniform configuration with the overall director determined by the boundary condition. On the other hand, the influence of the pressure tensor favors a radial director field. If $\kappa \ll 1$ N, even configurations with defects can be found, while for $\kappa > 1$ N the resulting director configurations are of the type shown in Fig. 4. As expected, for $\kappa \rightarrow \infty$ the same fourfold symmetry in the amount of reorientation is found that occurs in both the experiment and analytical calculations for small reorientation angles. For finite κ , however, the reorientation in the direction parallel to the orientation is smaller than that in the perpendicular direction.

Since this additional breaking of symmetry is not found in the experiment, one can conclude that $\kappa \gg 1$ N. The polarization patterns shown in Fig. 5 were calculated from the solution found for $\kappa = 50$ N using the Müller-matrix formalism [27]. For this and smaller values of κ , the asymmetry can hardly be detected visually.

V. CONCLUSIONS

A glassy nematic liquid crystal with an initially homogeneous alignment has been subject to photothermal excitation. Though the polarization of the incident laser beam was parallel to the nematic director, a reorientation of the alignment took place which was detected by polarization microscopy. The reorientation phenomena can be explained by stress-optical coupling, where the stress is caused by the locally inhomogeneous temperature field resulting from laser heating.

We developed a theoretical model based on an equation for the second rank alignment tensor which includes a coupling between the symmetric traceless part of the pressure tensor and the alignment. The order of magnitude of the stress-optical coupling coefficient has been estimated by comparison to well established equations for the isotropic and nematic phases. The coefficient is proportional to the ratio of a rotational viscosity to a shear viscosity. This equation was then specialized for a uniaxial alignment with a constant scalar order parameter.

For the application of the equation to the experimental situation, an expression for the pressure tensor was calculated starting from a local stability criterion and an appropriate ansatz for the temperature field. In order to mimic the kind of threshold behavior observed in the experiment, we introduced a cutoff at the boundary of the illuminated spot in two different ways: For an analytic calculation valid for small reorientation angles, the pressure tensor was taken to be zero outside the heated regime. In a numerical treatment the director field was fixed at the boundary of the heated region.

Both methods lead to similar director fields which exhibit the same symmetry that has been observed in the birefringence patterns. The predicted polarization patterns agree well with the experimental findings. A minor difference is found at the border between the heated and unheated area: The cutoff in the director field results in a boundary that is a bit too sharp, while the cutoff in the pressure tensor yields a more diffuse border rim. It should be possible to amend this shortcoming by introducing a spatial dependent elasticity coefficient $K(r)$, which is larger in the unheated regime than in the center.

From a quantitative point of view, the director field is determined by the ratio of the elastic constant K to the stress-optical coupling coefficient C_{np} . The calculations predict that in the present experiment this ratio is rather large and at least in the order of 10^2 N. This seems to be reasonable since it can be expected that the elastic constant is much larger in the glassy than in the liquid crystalline state.

ACKNOWLEDGMENTS

Partial financial support of this work by the Deutsche Forschungsgemeinschaft (DFG) via the SFB 335 "Anisotrope Fluide" is gratefully acknowledged.

-
- [1] P. Hartmann, Ph.D. thesis, Martin-Luther-Universität, Halle/Saale, 1990 (in German).
- [2] H.J. Eichler, G. Heppke, R. Macdonald, and H. Schmid, *Mol. Cryst. Liq. Cryst.* **223**, 159 (1992).
- [3] H.J. Eichler, R. Elschner, G. Heppke, R. Macdonald, and H. Schmid, *Mol. Cryst. Liq. Cryst.* **250**, 293 (1994).
- [4] H.J. Eichler, R. Elschner, G. Heppke, R. Macdonald, and H. Schmid, *Appl. Phys. B: Photophys. Laser Chem.* **61**, 59 (1995).
- [5] R. Elschner and R. Macdonald, *Mol. Cryst. Liq. Cryst.* **282**, 107 (1996).
- [6] H. Janeschitz-Kriegl, *Polymer Melt Rheology and Flow Birefringence, Polymers, Properties and Applications 6* (Springer, Berlin, 1983).
- [7] J.L. Ericksen, *Mol. Cryst. Liq. Cryst.* **7**, 135 (1969).
- [8] F.M. Leslie, *Mol. Cryst. Liq. Cryst.* **7**, 407 (1969).
- [9] H.J. Eichler and R. Macdonald, *Phys. Rev. Lett.* **67**, 2666 (1991).
- [10] S. Hess, *Phys. Lett.* **30A**, 239 (1969).
- [11] S. Hess, *Z. Naturforsch. A* **28**, 861 (1973).
- [12] F. Baas, P. Oudeman, H.F.P. Knaap, and J.J.M. Beenakker, *Physica A* **88**, 44 (1977).

- [13] D. Baals and S. Hess, *Z. Naturforsch. A* **40**, 3 (1985).
- [14] E. Leutheusser, *Phys. Rev. A* **29**, 2765 (1984).
- [15] E. Rössler, *Phys. Rev. Lett.* **65**, 1595 (1990).
- [16] W. Götze and L. Sjörgen, *Rep. Prog. Phys.* **55**, 241 (1992).
- [17] C. Selbmann, W. Witko, and H. D. Koswig (unpublished).
- [18] H.J. Eichler, R. Macdonald, and C. Dettmann, *Mol. Cryst. Liq. Cryst.* **174**, 153 (1989).
- [19] P.G. De Gennes and J. Prost, *The Physics of Liquid Crystals*, 2nd ed. (Clarendon, Oxford, 1993).
- [20] S. Hess, *Z. Naturforsch. A* **30**, 728 (1975).
- [21] C. Pereira Borgmeyer and S. Hess, *J. Non-Equilib. Thermodyn.* **20**, 359 (1995).
- [22] S. Hess, *Z. Naturforsch. A* **31**, 1034 (1976).
- [23] A. Kilian and S. Hess, *Liq. Cryst.* **8**, 465 (1990).
- [24] A. Kilian and S. Hess, *Mol. Cryst. Liq. Cryst.* **204**, 155 (1991).
- [25] A. Sonnet, A. Kilian, and S. Hess, *Phys. Rev. E* **52**, 718 (1995).
- [26] D. Grebe and R. Macdonald, *J. Phys. D* **27**, 567 (1994).
- [27] W.A. Shurcliff, *Polarized Light* (Harvard University Press, Cambridge, MA, 1966).